N and S co-doped RGO as effective counter electrode for quantum dot sensitized solar cells

XUAN JI, MAOLIN ZHANG*, PENG ZHONG, DONGYAN ZHANG, PENG SUN, YUAN WANG, ZHIMIN LI
School of Advanced Materials and Nanotechnology, Xidian University, Xi'an, 710071, China

Counter electrode (CE) is used to catalyze the reduction of oxidized species in an electrolyte for quantum dot sensitized solar cells (QDSSCs). Carbon based materials were considered as excellent candidates for CEs. In this work, N and S co-doped reduced graphene oxide (RGO) was prepared by simple one-step hydrothermal synthesis to increase the number of active catalytic site. XPS was used to analyze surface chemistry state of doped RGO in depth. TiO_2/CdS/CdSe based QDSSCs using as-prepared CE showed enhanced photovoltaic performance with power conversion efficiency of 2.3%, far superior to that of a cell with undoped RGO. EIS and Tafel-polarization measurements were used to investigate electrocatalytic activity of as-prepared CEs. Improved photovoltaic performance can be attributed to N and S co-doping, making surrounding carbon atoms active. This is beneficial in providing more active sites for S_n^{2-}/S^{2-} redox couple.

(Received September 11, 2018; accepted June 14, 2019)

Keywords: QDSSCs, Counter electrode, N and S co-doped RGO, Electrocatalytic activity

1. Introduction

Quantum dot sensitized solar cells (QDSSCs) have attracted much attention in recent years because of their low cost, easy fabrication and high theoretical power conversion efficiency (PCE) [1]. A typical structure of QDSSCs was constructed as the sandwich structure, including a photoanode, an electrolyte and a counter electrode (CE) [2]. The counter electrode serves as a catalyst, and enables to transfer the electrons from an external circuit into the redox electrolyte of QDSSCs, catalyzing the reduction of oxidized species within it [3-4]. Therefore, CEs with a high electrocatalytic activity towards electrolyte regeneration and excellent electrical conductivity help to improve the PCE of QDSSCs. Moreover, long-term chemical stability and low production cost are also required for practical applications.

First, noble metals (especially Pt) were widely used as CEs for QDSSCs according to the results of DSSCs. However, it has been confirmed that its electrocatalytic activity can be adversely affected, due to the fact that Pt might dissolve in the electrolyte, hence decreasing the PCE [5-10]. Moreover, they are expensive materials, limiting their wide applications.

Then, metal sulfides such as Cu_xS [7, 11], PbS [8], CoS [9], NiS [6] and FeS_x [5] with high electrocatalytic activity for polysulfide redox reaction were introduced as CEs. Among then, Cu_2S built on a metal foil substrate in a polysulfide electrolyte showed superior performance. However, such a preparative method suffers from continual corrosion, leading to mechanical instability. Kamat et al. [10] exposed a small foil of 90/10 Cu/Zn brass to a polysulfide solution and found that the material completely disintegrated after one week. Moreover, it was reported that Cu_2S CEs poison the photoanode surface, gradually decreasing the open-circuit voltage (V_{oc}) and short-circuit current density (J_{sc}) [9].

Apart from noble metals and metal sulfides, carbon materials including graphene, graphite, carbon nanotubes and activated carbon were considered as excellent candidates for CEs because of their competitive cost and good electrocatalytic properties. Much effort has been devoted to carbon CEs with various structures to improve the photoelectric characteristics of solar cells [12-17]. Generally, two typical methods are widely used: (i) developing composites and (ii) doping. Carbon-based composites often consist of metal sulfides with combined advantages of each component. The electrochemical properties of graphene/MoS [18] and graphene/Cu_xS [10-11] were extensively studied.

Another effective method is to directly improve the intrinsic electrochemical properties of carbon-based CEs themselves. It has been reported that N-doped carbon materials show high electrocatalytic properties. Zhu et al. [19] prepared N-doped hollow carbon nanoparticles (N-HCNPs) as CEs in QDSSCs, achieving a PCE of 2.7%. The excellent electrocatalytic activity of N-HCNPs arose form N-doping that introduced many active sites. Then, N-doped mesoporous carbon was used as the CE in Zn-Cu-In-Se QDSSCs in Zhong's work [4]. The PCE was as high as 12.07% as certified by CPVT, confirming the superior catalytic activity.

Graphene has many unique properties such as excellent conductivity, low cost and ease modification.

However, it is usually difficult to satisfy the demands of CEs by perfectly structured graphene due to strong π-π interaction, which significantly limited the amount of active defective site [20]. Doping can help to enhance the electron density of graphene and increase the electrical conductivity. In this study, N and S co-doped reduced graphene oxide (RGO) was prepared by a simple one-step hydrothermal synthesis to increase the number of active defective sites. The results indicate that the N/S co-doped RGO CE exhibits good potential application in QDSSCs.

2. Experiments

2.1. Preparation of CEs

Pure RGO and N/S co-doped RGO CEs were prepared by using hydrothermal method. First, graphene oxide (GO) was synthesized via improved Hummer method as reported in ref. [21]. Thiourea (CH_4N_2S, Paini Technology, AR) was used as the source of sulfur and nitrogen. Then, GO was complexed with thiourea in deionized water with increasing mass of thiourea. The samples were denoted as RGO-Tx, standing for the doping source originating from thiourea, where x (x = 5, 10, or 15) is the mass fraction of thiourea. Then, the solution was transferred to an autoclave and kept at 180 °C for 24 h. The resulting composite was thoroughly washed by centrifugation and resuspension.

Finally, CEs were prepared by printing the prepared powders onto a nickel foam. This powder was mixed with 1 wt.% PTFE binder. Because of good chemical stability and excellent electrical conductivity, a nickel foam was used as the support substrate for preparing CEs for QDSSCs.

2.2. Cell fabrication

The photoelectrochemical cell of QDSSCs was constructed as a sandwich structure [2]. Mesoporous TiO_2 films were prepared using the doctor blade method with TiO_2 paste printed onto the FTO, followed by sintering at 500 °C for 2 h. Then, CdS/CdSe co-sensitized QDs were deposited on the prepared mesoporous TiO_2 film by using successive ionic layer adsorption and reaction and chemical bath deposition methods respectively, as reported in ref. [1-3]. The active area of this device was about 0.2 cm^2. The polysulfide electrolyte used in this study was composed of 1 M S and 1 M Na_2S in deionized water.

2.3. Characterization of CEs and QDSSCs

X-ray diffraction (XRD, D8 Advance, Bruker, Germany) was used to characterize the phase structure. The morphologies were observed using a scanning electron microscope (SEM, JSM-7500F, Jeol, Japan). The surface components of prepared materials were characterized by X-ray photoelectron spectroscopy (XPS, Axisultra, Kratos, UK) with Al Kα radiation. The binding energies were calibrated using the C1s hydrocarbon peak at 284.8 eV. The wettability of polysulfide electrolyte against the CEs was tested by a contact angle measurement instrument (JC2000C1, Powereach, China). Electrochemical impedance spectra (EIS) and Tafel-polarization were carried out using an electrochemical workstation (CHI660E, Chinstruments, China). The photovoltaic properties of QDSSCs were measured using a Zahner CIMPS-II photoelectrochemical system under AM 1.5 simulated sunlight with a power density of 100 mW/cm^2.

3. Results

3.1. Photovoltaic performance

The current density-voltage (J-V) characteristics of QDSSCs obtained using various CEs are shown in Fig. 1. The QDSSCs with RGO CE showed a low PCE of 0.9 %. Notably, this obtained PCE is on the same level as previously reported results [22-23]. As expected, the introduction of thiourea to RGO CEs increased the PCE compared with pure RGO. The addition of 10 wt.% thiourea to RGO CE increased the PCE from 0.9% to 2.1%. The PCE improved mainly because of the co-doping of N and S, increasing the FF from 43.9% to 56.7% and J_{sc} from 4.6 to 7.3 mA/cm^2.

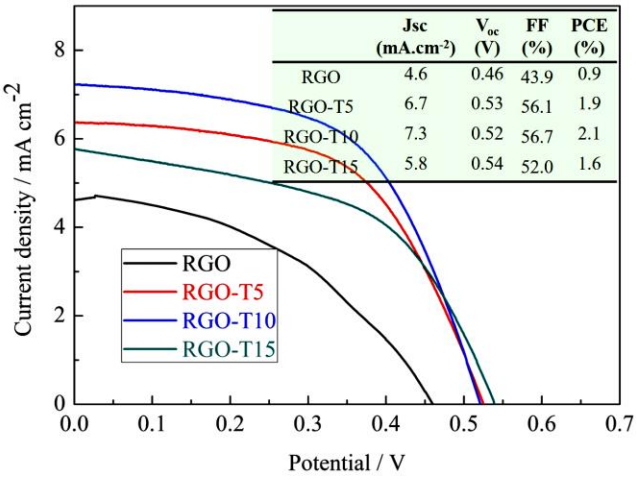

Fig. 1. Photocurrent-voltage characteristics of QDSSCs based on various CEs

3.2. Structure, morphology and surface state

XRD was used to confirm the phase structure of different CEs, as shown in Fig. 2. No essential difference was observed between RGO and N/S co-doped RGO, indicating that N and S co-doping probably did not affect the RGO layers. SEM were used to confirm the morphology of different CEs, as shown in Fig. 3. The layered structure of undoped and doped RGO sheets is apparent from the micrograph, as reported by Huang [23].

XPS was performed on the sample RGO and RGO-T10 to determine the surface chemical composition and electronic state of the as-prepared samples. As shown in Fig. 4 (A), the elemental composition was analyzed from the XPS survey spectrum, indicating the presence of

C, N, S and O in the sample. However, N and S could not be found in RGO. This indicates the successful synthesis of N and S co-doped RGO. The relative ratios of C, O, N and S in RGO-T10 are 83.5, 10.3, 4.1 and 2.1 at%, respectively. The proportion of N to S in this sample (N/S = 4.1/2.1) is almost equivalent to that in the source (CH_4N_2S, N/S =2/1). Similarly, the relative ratios of N and S in RGO-T5 are 1.4 and 0.6 at%, respectively.

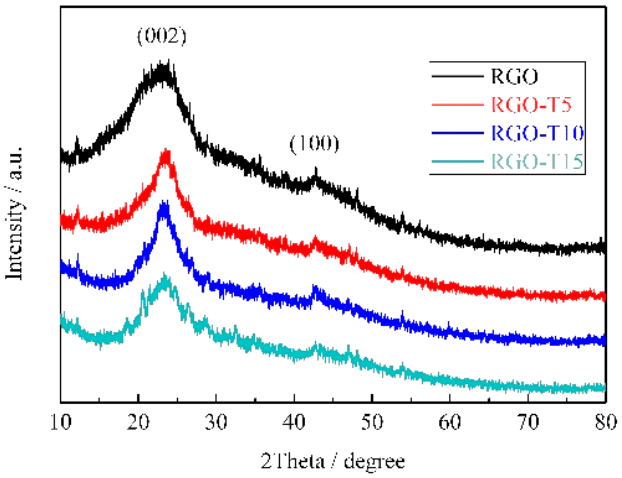

Fig. 2. XRD patterns of various CEs

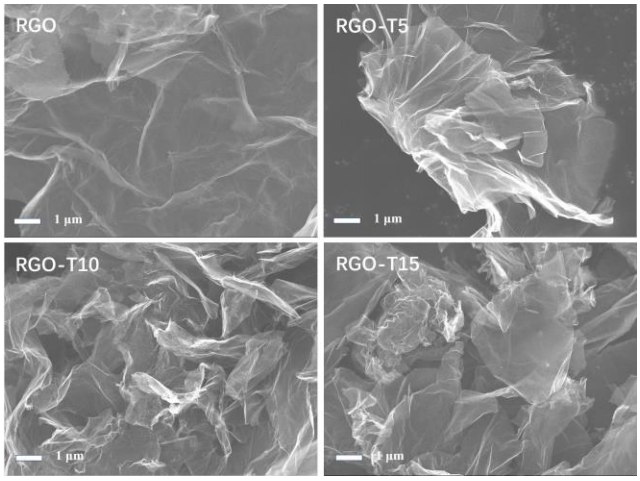

Fig. 3. SEM images of various CEs

The high-resolution XPS spectra of C1s, N1s and S2p are shown in Fig. 4 (B), (C) and (D), respectively. As can be seen, the C 1s peak could be deconvoluted to three peaks centered at 284.8, 286.4 and 288.9 eV [11, 24]. The peak at 284.8 eV can be assigned to graphitic carbon (C-C) originating from the graphene [11, 24]. The peaks centered at 286.4 eV and 288.9 eV can be assigned to surface oxygen, sulfur and nitrogen groups (designated as C-O/C-N/C-S and O=C-O, respectively) [25-26]. This result confirms that most carbon atoms are graphite carbons (sp2 carbons), and the N and S were co-doped into the graphite-like layers [4].

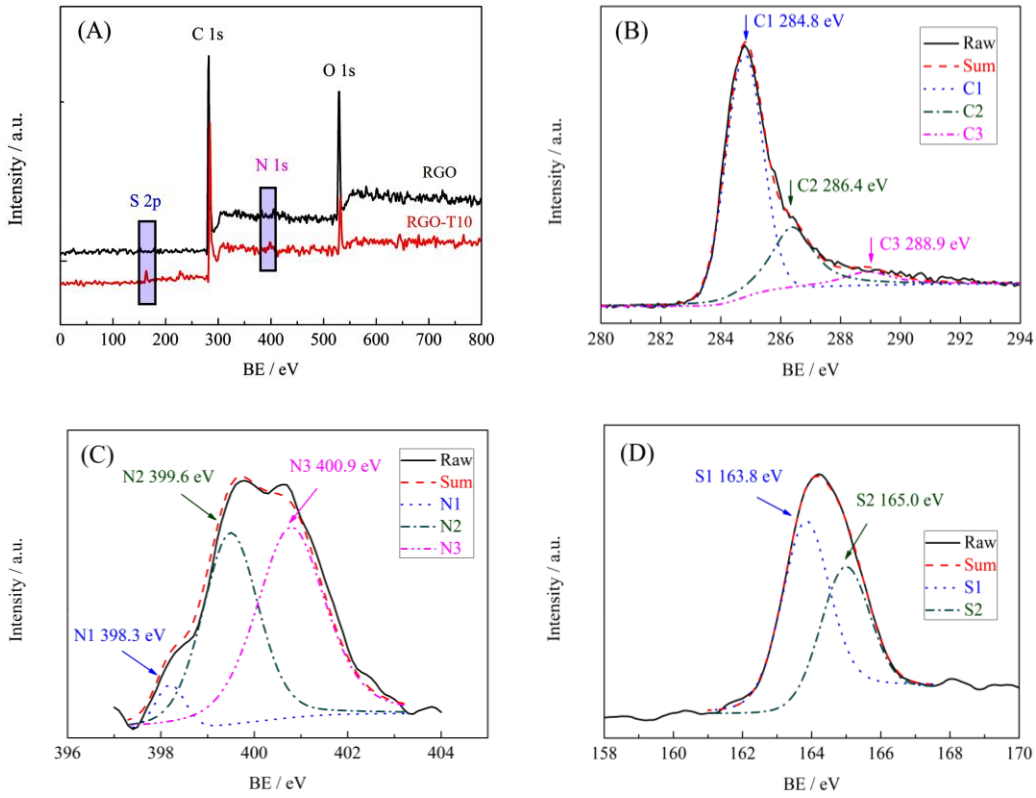

Fig. 4. XPS survey spectra of RGO and RGO-T10 (A), high-resolution C 1s (B), N 1s (C) and S2p (D) spectra of RGO-T10 sample

The N1s spectrum was successfully deconvoluted into three different peaks, corresponding to three nitrogen configurations such as pyridinic-N (N1, 398.3 eV), pyrrolic-N (N2, 399.6 eV) and quaternary-N (N3, 400.9 eV)) [27-28]. As reported by Zhong [4], the pyridinic-N and pyrrolic-N atoms are located at the edges of graphite-like layers. The presence of pyridinic-N and pyrrolic-N atoms introduces more disorder to the carbonaceous material, beneficial in improving the catalytic properties of CEs in polysulfide electrolyte. Moreover, the quaternary-N played an important role in increasing the electrical conductivity of graphene [28], because the carbon atoms adjacent to nitrogen produce a higher positive charge [29].

The wettability of polysulfide electrolyte on CEs is shown in Fig. 5. It can be observed that the contact angle of polysulfide electrolyte against RGO-T10 is 55°, whereas it is as high as 66° for RGO. Because of the co-doping of N and S, the defects in graphene sheet structure increased. Therefore, it can be inferred that the active defective site is beneficial in improving the wettability. Materials with excellent wettability have been reported to be beneficial for the promotion of absorption of electrolyte, further increasing the conductivity [30]. This result is also consistent with the photocurrent-voltage characteristics shown in Fig. 1, as the J_{sc} clearly increased for the resulting QDSSCs with N/S co-doped RGO CEs.

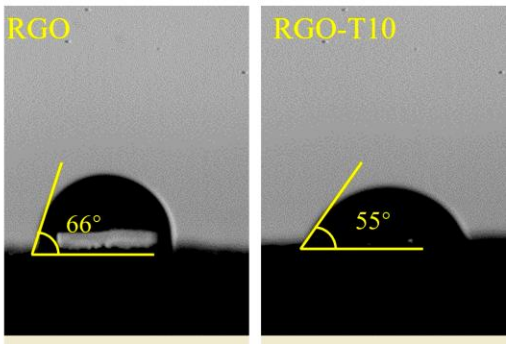

Fig. 5. Wettability of polysulfide electrolyte against RGO and RGO-T10 samples

3.3. Electrochemical performances

EIS was used to further investigate the catalytic activity of CEs in QDSSCs, as shown in Fig. 6(A). One semicircle and oblique line were observed in the Nyquist plot for each CE, related to different resistances. The charge transfer resistance (R_{ct}) corresponding to the charge exchange between CEs and polysulfide electrolyte was derived from the semicircle in the Nyquist plots. It can be found that the R_{ct} of all the doped RGO CEs are smaller than the undoped. Particularly, the sample RGO-T10 showed the lowest R_{ct}, as low as 0.45 Ω/cm^2. A decrease in R_{ct} indicates an increase in the electrocatalytic activity of CE, reflecting an acceleration of electron transfer process at the electrolyte and CE interface [7]. Accordingly, a lower R_{ct} indicates a more effective reduction of S_n^{2-} to S^{2-}, improving the photovoltaic performance [4]. Therefore, the sample RGO-T10 with the lowest R_{ct} showed the highest J_{sc}.

Tafel measurements were performed to further evaluate the improvement of catalytic activity of prepared CEs, as shown in Fig. 6(B). The exchange current density (J_0) is directly related to the electrocatalytic activity of CE. The relationship between J_0 and R_{ct} can be expressed as follows [3],

$$J_0 = RT/nFR_{ct} \quad (1)$$

where R, T, n and F are the universal gas content, temperature, number of electrons contributing to the charge transfer at the interface, and Faraday constant, respectively. Therefore, a low R_{ct} indicates a high exchange current density. Then, it can be found that an increasing trend of J_0 was obtained in the Tafel curves, consistent with the variation trend of R_{ct} in EIS.

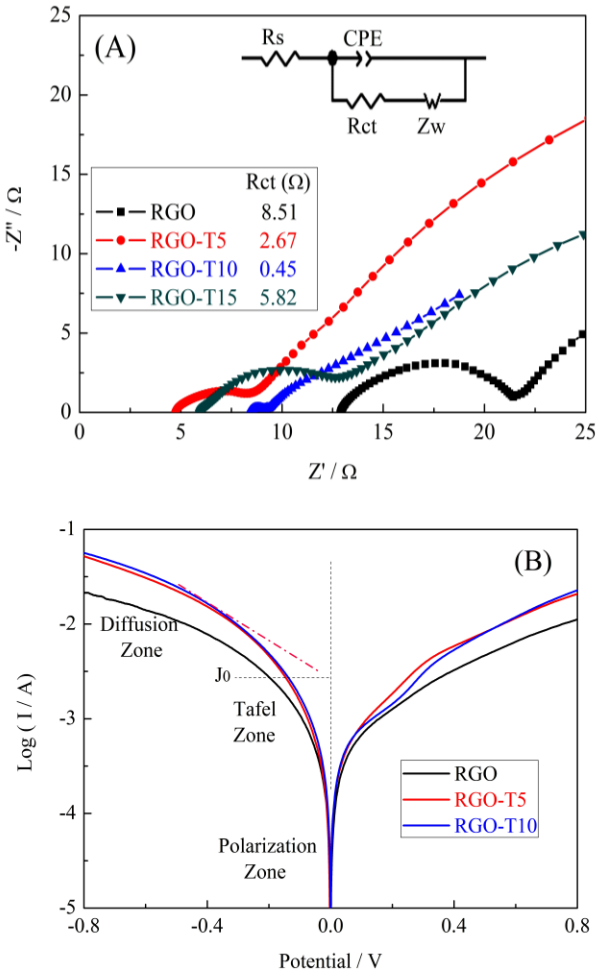

Fig. 6. Electrochemical properties of different CEs, EIS (A) and Tafel polarization (B)

Further, the RGO-T10 CE sample was treated at different temperatures from 180 to 220 °C when it was prepared via the hydrothermal method. It was found that no obvious difference was observed in V_{oc} (0.53 ± 0.1 V) and J_{sc} (7.2 ± 0.1 mA/cm^2). However, the QDSSCs with CE prepared at 200 °C showed the highest PCE, as high as 2.3% as shown in Fig. 7, probably because of the increase in FF from 50.8% to 59.6%. Similarly, electrochemical performances were obtained by EIS and CV, as shown in the inset of Fig. 7. It can be found that the RGO-T10 CE sample treated at 200 °C showed the lowest R_{ct} (0.2 Ω/cm^2) and highest $|I_{red}|$ (86.8 mA). Therefore, the experimental results indicate that an effective CE can be obtained by selecting a suitable hydrothermal temperature.

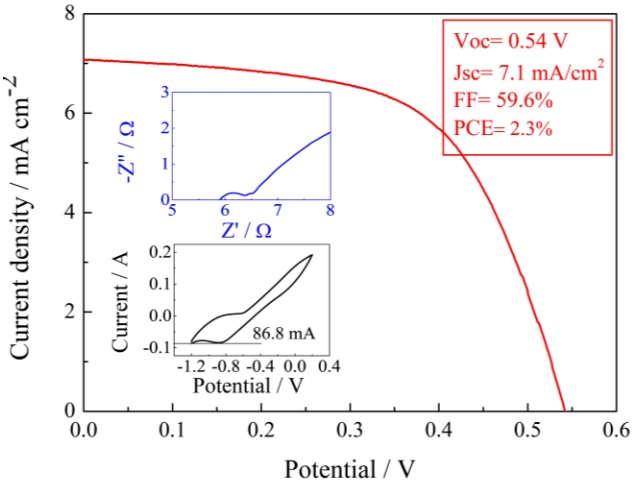

Fig. 7. Photocurrent-voltage characteristics of QDSSCs based on RGO-T10 treated at 200 °C. The electrochemical properties (EIS and CV) are shown in the inset

4. Conclusions

In this work, N and S co-doped RGO materials were successfully prepared by a simple one-step hydrothermal synthesis and used as CEs in QDSSCs. Thiourea was used as the source of sulfur and nitrogen. By optimizing the thiourea content and treatment temperature, the fabricated cell devices achieved a PCE of 2.3% (J_{sc} = 7.1 mA/cm^2, Vo_c = 0.54 V, FF = 59.6%) for TiO_2/CdS/CdSe-based QDSSCs, much higher than undoped RGO electrodes. The electrochemical performances showed that the R_{ct} of co-doped electrode towards the polysulfide electrolyte significantly decreased compared with undoped electrode. The better performance of prepared electrode can be mainly attributed to the higher electrocatalytic activity because of N and S co-doping, introducing many active sites in the graphite-like layers.

Acknowledgements

This work was supported by the National Natural Science Foundation of China (grant numbers 61701369 and 11604250); the Natural Science Basic Research Plan in Shaanxi Province of China (grant numbers 2018JM6070 and 2018JM5060); the Fundamental Research Funds for the Central Universities (grant number JB181407).

References

[1] Shixun Wang, Jianjun Tian, RSC Advance **6**, 90082 (2016).
[2] Meidan Ye, Xiaoyue Gao, Xiaodan Hong, Qun Liu, Chunfeng He, Xiangyang Liu, Changjian Lin, Sustainable Energy Fuels **1**, 1217 (2017).
[3] Insung Hwang, Kijung Yong, Chemelectrochem **2**, 634 (2015).
[4] Shuang Jiao, Jun Du, Zhonglin Du, Donghui Long, Wuyou Jiang, Zhenxiao Pan, Yan Li, Xinhua Zhong, Journal of Physical Chemistry Letters **8**, 559 (2017).
[5] Feng Liu, Jun Zhu, Yi Li, Junfeng Wei, Mei Lv, Yafeng Xu, Li Zhou, Linhua Hu, Songyuan Dai, Journal of Power Sources **292**, 7 (2015).
[6] Chandu Gopi, S. Srinivasa Rao, Soo-Kyoung Kim, Dinah Punnoose, Hee-Je Kim, Journal of Power Sources **275**, 547 (2015).
[7] Shankara Sharanappa Kalanur, Sang Youn Chae, Oh Shim Joo, Electrochimica Acta **103**, 91 (2013).
[8] Zion Tachan, Arie Zaban, Journal of Physical Chemistry C **115**, 6162 (2011).
[9] Matthew Faber, Kwangsuk Park, Miguel Cabán-Acevedo, Pralay K. Santra, Song Jin, Journal of Physical Chemistry Letters **4**, 1843 (2013).
[10] James G Radich, Ryan Dwyer, Prashant V. Kamat, Journal of Physical Chemistry Letters **2**, 2453 (2011).
[11] Yanyan Zhu, Huijuan Cui, Suping Jia, Jianfeng Zheng, Pengju Yang, Zhijian Wang, Zhenping Zhu, Electrochimica Acta **208**, 288 (2016).
[12] Xiangtong Meng, Chang Yu, Xuedan Song, Yang Liu, Suxia Liang, Zhiqiang Liu, Ce Hao, Jieshan Qiu, Advanced Energy Materials **5**, 1500180 (2015).
[13] Xiangtong Meng, Chang Yu, Xuedan Song, James Iocozzia, Jiafu Hong, Matthew Rager, Huile Jin, Shun Wang, Longlong Huang, Jieshan Qiu, Zhiqun Lin, Angewandte Chemie **130**, 4772 (2018).
[14] Chang Yu, Xiangtong Meng, Xuedan Song, Suxia Liang, Qiang Dong, Gang Wang, Ce Hao, Xichuan Yang, Tingli Ma, M. Ajayan, Jieshan Qiu, Carbon **100**, 474 (2016).
[15] Xiangtong Meng, Chang Yu, Xuedan Song, Zhiqiang Liu, Bing Lu, Ce Hao, Jieshan Qiu, Journal of Materials Chemistry A **5**, 2280 (2017).
[16] Xiangtong Meng, Chang Yu, Bing Lu, Juan Yang, Jieshan Qiu, Nano Energy **22**, 59 (2016).
[17] Xiangtong Meng, Chang Yu, Xuepeng Zhang, Longlong Huang, Matthew Rager, Jiafu Hong,

Jieshan Qiu, Zhiqun Lin, Nano Energy **54**, 138 (2018).
[18] Miaomiao Zhen, Fengyan Li, Ran Liu, Chunli Song, Lin Xu, X. Z. Luo, Journal of Photochemistry and Photobiology A: Chemistry **340**, 120 (2017).
[19] Jianhui Dong, Suping Jia, Jiazang Chen, Bo Li, Jianfeng Zheng, Jianghong Zhao, Zhijian Wang, Zhenping Zhu, Journal of Materials Chemistry **22**, 9745 (2012).
[20] Hui Bi, Houlei Cui, Tianquan Lin, Fuqiang Huang, Carbon **91**, 153 (2015).
[21] S. Hummers, E. Offeman, Journal of the American Chemical Society **80**, 1339 (1958).
[22] P. Parand, M. Samadpour, A. Esfandiar, A. I. Zad, ACS Photonics **1**, 323 (2014).
[23] H. D. Liu, J. L. Zhang, D. D. Xu, L. H. Huang, S. Z. Tan, W. J. Mai, Journal of Solid State Electrochemistry **19**, 135 (2015).
[24] I-Ping Liu, Hsisheng Teng, Yuh-Lang Lee, Journal of Materials Chemistry **44**, 23146 (2017).
[25] Manikantan Kota, Xu Yu, Sun-Hwa Yeon, Hae-Won Cheong, Ho Seok Park, Journal of Power Sources **303**, 372 (2016).
[26] Tongye Wei, Xiaolin Wei, Yong Gao, Huaming Li, Electrochimica Acta **169**, 186 (2015).
[27] Taiwo Odedairo, Jun Ma, Yi Gu, Wei Zhou, Jian Jin, X. S. Zhao, Zhonghua Zhu, Nanotechnology **25**, 495604 (2014).
[28] Junghoon Yang, Mi Ru Jo, Myunggoo Kang, Yun Suk Huh, Hyun Jung, Yong-Mook Kang, Carbon **73**, 106 (2014).
[29] Kuanping Gong, Feng Du, Zhenhai Xia, Michael Durstock, Liming Dai, Science **323**, 760 (2009).
[30] Dong Ye, Yao Yu, Jie Tang, Lin Liu, Yue Wu, Nanoscale **8**, 10406 (2016).

*Corresponding author: mlzhang@xidian.edu.cn